JOINT INSTITUTE FOR NUCLEAR RESEARCH
Frank Laboratory of Neutron Physics

FINAL REPORT ON THE
SUMMER STUDENT PROGRAM

Study of structure and dynamics of nanomaterials as a drug delivery

Supervisor:
PhD. Dorota Chudoba

Students:
Buzrikov Shovkat, Uzbekistan
Institute of Nuclear Physics,
Jumanov Abror, Uzbekistan,
Jizzax State Pedagogical Institute

Participation period:
July 07 – August 31

Dubna, 2019

CONTENTS

1. Description of the project 3

2. Theoretical introduction to Neutron spectroscopy.....3

3. Methods 9

3.1 X-ray diffraction.....9

3.2 Inelastic neutron scattering.....10

3.3 Neutron diffraction.....13

4. Experiment 15

4.1 X-ray diffractometer.....15

4.2 NERA spectrometer.....17

5. Results and discussion 18

6. Conclusions 24

7. Acknowledgement 24

8. References 26

1. Description of the project

We were the participant of Summer Student Program in Joint Institute for Nuclear Research (JINR) in Dubna from 07.07.2019 to 31.08.2019. During the practice course in the Frank Laboratory of Neutron Physics (FLNP) headed by dr. Dorota Chudoba, we have obtained the basic knowledge in neutron methods which are used in studies of condensed matter and also acquainted with the history of JINR. We have visited the Reactor IBR-2 and other laboratories in JINR (FLNP, DLNP, FLNR) where we learned about their scientific activity.

The theme of our work was to study structure and dynamic of nanomaterials designed for drug delivery. The main purpose of this work was to examine various physical and chemical processes occuring in matter as a result of interaction with neutrons and to evaluate changes is the properties of the tested samples under the influence of neutrons and X-ray radiation. Experiments were performed in FLNP with using NERA spectrometer and X-ray diffractometer. The experiments results were also analyzed in FullProf and HighScore programs.

2. Theoretical introduction to Neutron spectroscopy

In 1935 Professor James Chadwick was awarded the Nobel Prize in Physics for the discovery of the neutron. In 1942 Enrico Fermi showed that neutrons from fission of the uranium nucleus could support a controlled chain reaction. Earlier in 1938 he won the Nobel Prize in Physics for the discovery that slowed-down neutrons more readily interact with matter and could be used to detect the positions and motions of atoms. At the end of the Second World War the researchers in the USA gained access to the large neutron fluxes delivered by first nuclear reactors. The first neutron diffraction experiments were carried out in 1945 by Ernest Wollan at the Graphite Reactor in the Oak Ridge National Laboratory, USA. Together with Clifford Shull they established the basic principles of this experimental technique and successfully applied it to study different materials. Cliff Shull and Bertram Brockhouse demonstrated that the directions in which neutrons are “elastically” scattered without changing energy provide information on the position and arrangement of atoms. In 1994 Shull and Brockhouse received the Nobel Prize in Physics for their pioneering ideas and contributions to the development of neutron scattering techniques. Over the past fifty years a constantly increasing number of scientists from the fields of physics, chemistry, biology, materials science, geology and others have been turning to neutron scattering methods to find the answers to the most complicated problems in their fields of research[1].

The neutron is a particle without electric charge and with a mass about 1,0087 u ($1{,}675*10^{-27}$kg). Neutron consists of three quarks: two quarks *d* with the charge about – 1/3 and the one *u* with a charge +2/3 Neutron has a spin $\mathbf{s=\frac{1}{2}}$

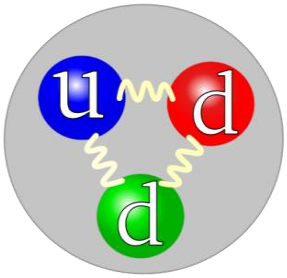

Fig.1. The scheme of neutron [2].

Neutron was discovered by James Chadwick in 1932. The α-particles beam was fired on beryllium nucleus, which gave the neutron and the carbon nucleus:

$$^{9}_{4}Be + {}^{4}_{2}He \rightarrow {}^{12}_{6}C + {}^{1}_{0}n + 5{,}7\ MeV$$

The obtained neutrons collided with paraffin foil and ejected the protons from it. The protons were recorded by Geiger-Muller counter.

Neutrons are stable only in stable atomic nucleus. Free neutrons are labile and they decay with the mean lifetime 881.5±1.5 s (about 14 minutes, 42 seconds) [3] into a proton (p), an electron (e) and an antineutrino ($\tilde{\nu}_e$). This process is named β decay:

$$n \rightarrow p^{+} + e^{-} + \tilde{\nu}_e$$

Neutron has the wave-particle properties. The de Broglie relation describes the neutron wavelengths: [4]

$$\lambda_n = \frac{h}{m_n \vartheta_n} = \frac{h}{\sqrt{2 m_n E_n}}$$

According to their energy there are different categories of neutrons (Table1.):

- Epithermal neutrons
- Thermal neutrons
- Cold neutrons
- Ultracold neutrons

Table 1. Characteristics of Neutrons at Selected Energies [5]

Quantity	Unit	Definition	Ultracold	Cold	Thermal	Epithermal
Energy E	meV[a]		0.00025	1	25	1000
Temperature T	K	E/k_B	0.0029	12	290	12,000
Wavelength λ[b]	Å	$h/(2mE)^{1/2}$	570	9.0	1.8	0.29
Wave vector k[c]	$Å^{-1}$	$(2mE)^{1/2}/\hbar$	0.011	0.7	3.5	22
Velocity v[d]	m/s	$(2E/m)^{1/2}$	6.9	440	2200	14,000

[a] 1 meV = 1.6022×10^{-15} erg, the energy required to raise a proton up to a potential of 1 mV.
[b] λ (Å) = 9.0446 [E (meV)]$^{-1/2}$.
[c] k ($Å^{-1}$) = 0.69469 [E (meV)]$^{1/2}$.
[d] v (m/s) = 437.39 [E (meV)]$^{1/2}$.

Neutron sources

There are different types of neutron sources:

- Small neutron sources
- Nuclear fission
- Neutron sources based on particle accelerators

The γ radiation is used in *small neutron sources.* The γ quantum incident on a beryllium nucleus giving its isotope and neutron:

$$^{9}_{4}Be + \gamma \rightarrow {}^{8}_{4}Be + {}^{1}_{0}n - 1{,}66\ MeV$$

In *nuclear fission* an ^{235}U absorbs thermal neutron and decays into two smaller nuclei and gives on average 2,5 neutrons (Figure 2.) with releasing 200MeV of energy:

$$^{1}_{0}n + {}^{235}_{92}U \rightarrow 2\ nuclei + 2{,}5\ {}^{1}_{0}n + 200\ MeV$$

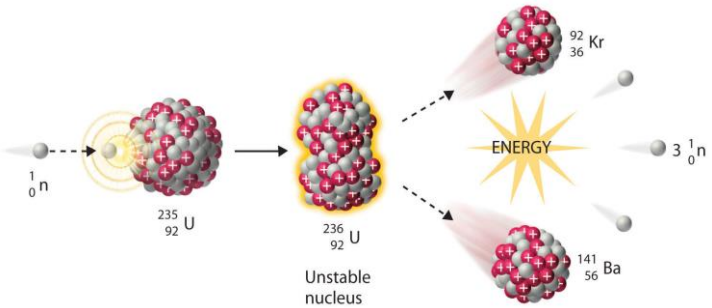

Fig.2. An example of nuclear fission of ^{235}U which decays into ^{141}Ba and ^{92}Kr [6].

The obtained neutrons have the energies around 1 MeV. This chain reactions proceeds in neutron reactors. Types of reactors: a stationary and pulsed. In a stationary reactor from 2,5 neutrons 1 is needed to maintain the chain reactions 0,5 is absorbed by the construction elements and there is one which can be used in research.

The second type of reactor is a pulsed reactor. Example of this kind of reactors is IBR reactor working at FLNP JINR. The first pulsed reactor was built in FLNP JINR in 1960. In these days in FLNP JINR is working IBR-2 reactor which is a fast reactor with periodic action (Fig.3). Its core is made by 69 fuel assemblies filled by PuO_2. Those assemblies are directly cooled by liquid sodium. The core is surrounded by 5 stationary reflectors and the sixth movable reflector. This movable reflector consists of: the min movable reflector and the auxiliary movable reflector. They rotate against each other with different rotating speed. While two reflectors are near the core the neutrons are refluxed to the core and it generates a power pulse. When the reflectors move away the power of reactor decreases. The whole reactor is also cooled by liquid sodium and covered by two biological shields.

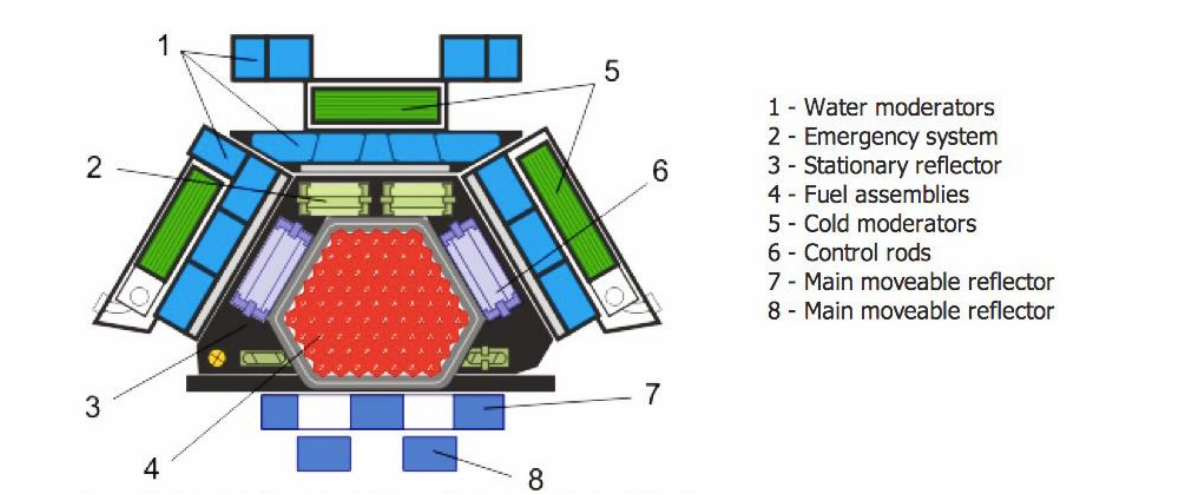

Fig.3. The scheme of reactor core of IBR-2 and its description [7].

There are also *particle accelerators*, which can be neutron sources. A particle beam is fired on heavy nucleus. For example, deuterons are accelerated to the energy of 100keV and they incident on a target made of TiT_2. In this process we obtain the nuclei of helium and neutrons:

$$ {}^{2}_{1}D + {}^{3}_{1}T \rightarrow {}^{4}_{2}He + {}^{1}_{0}n + 17{,}6\ MeV $$

When there is a target built from heavy chemical elements like Pb, W, Ta and very fast electron beam is fired on it, it provides a photonuclear reaction. Inhibitory electrons produce the γ quantum fluxes. This kind of radiation is called Bremsstrahlung. When these γ quants interact with the nuclei of a target, the neutrons are formed (γ, n). This source gives short and pulsed neutron beams. The accelerator, which uses that type of neutron source, is IREN in Dubna.

And the last example of neutron source based on a particle accelerator is the *spallation process.* It takes place in the nuclear reaction between the high-energy particles and heavy elements. Firstly the intense beam of protons is focused onto a target (e.g. uranium). The nucleus of the target becomes excited and there are multiple intra-nuclear reactions taking place. As a result nucleus produces the very high-energy neutrons. Finally, the nucleus throws out neutrons, protons, deuterons, α particles, photons and neutrinos. In those reactions one proton and one heavy nucleus create many neutrons.

To sum up it is important to use the neutron source, which produces many neutrons but also does not release much energy so that it is needed to optimize the neutron production.

Neutron interaction with matter

When a neutron is near the nucleus it could be:

- Absorbed by nucleus and excited it. After that nucleus could: emit γ quantum, undergo fission or throw away α particles, protons etc.
- Scattered by the nucleus that changes its energy and direction movement.

When the sample is under neutron beam $Ø_0$ and $I_s$is the number of scattering acts and I_a is the number of absorbing acts, the cross section for scattering σ_s and absorption σ_a are given by equations:

$$I_s = Ø_0 \sigma_s$$
$$I_a = Ø_0 \sigma_a$$

The σ_s and σ_a are measured in barns (1 barn = 10^{-28} square meter). The differential cross section for neutron scattering $\frac{d\sigma}{d\Omega}$ describes the probability that the scattered neutron can be detected at given angle Ω and will be found in the solid angle $d\Omega$. A double differential cross section describes the probability that the neutron will leave the sample at a given angle Ω and will be found in the solid angle $d\Omega$ and its energy will be changed from $\hbar\omega$ to $\hbar(\omega + d\omega)$. That gives an equation:

$$\sigma_s = \int d\Omega \frac{d\sigma}{d\Omega} = \int d\omega \int d\Omega \frac{d^2\sigma}{d\Omega d\omega}$$

Neutrons interact with nuclei by nuclear and magnetic forces. For nuclear forces the potential impact between neutron and nucleus is given by the Fermi pseudopotential, which is given by equation:

$$V(\vec{r}) = \frac{2\pi\hbar^2}{m} \sum_i b_i \delta(\vec{r} - \overrightarrow{R_i})$$

where b_i is the scattering length, R_i is the position of nucleus *i*in a sample and $\vec{r}$ is the position of a neutron. The mass of a neutron is given by *m* and δ is the Dirac delta. This is summed over every nuclei taking part in scattering. The scattering length is the base parameter, which describes the interaction between neutron and nucleus and it depends on the isotope and the relative spin orientation of each other. The average value of $<b_i>$ for every isotopes and spin orientations is named coherent scattering length $b_i^{coh} = <b_i>$. The average square variation of b_i is the incoherent scattering length:

$$b_i^{inc} = \sqrt{< b_i^2 > - < b_i >^2}$$

The scattering lengths for chosen elements and their isotopes are shown in Figure 4.

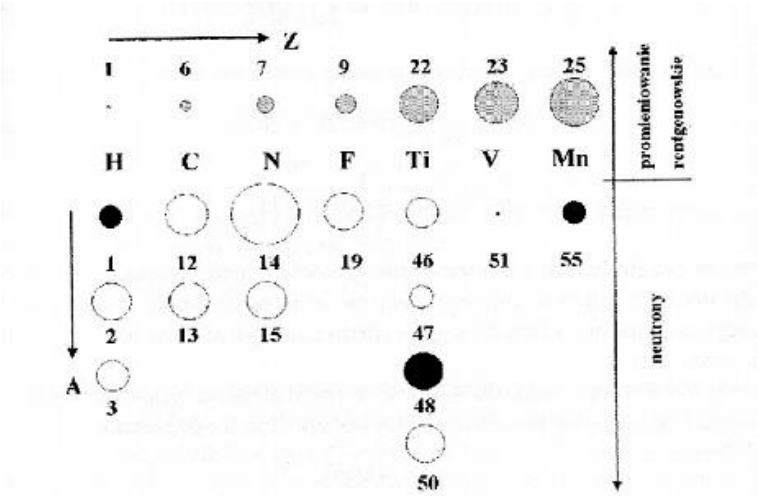

Fig.4. The comparison of the scattering lengths proportional to the diameter of circles for X-rays and neutrons. The black circle means the negative scattering lengths [8].

Opposite to x-ray scattering, the length scattering for neutrons depends irregularly to the Z number of an element and it depends of its isotopes. However, in the sample there is a mixture of isotopes, it means that it has both coherent and incoherent scattering length. The cross sections for the coherent and incoherent scattering will be:

$$\sigma_{coh} = 4\pi < b >^2$$

$$\sigma_{inc} = 4\pi(< b^2 > - < b >^2)$$

Relatively and the total cross section will be the sum of the coherent and incoherent cross section:

$$\sigma = \sigma_{coh} + \sigma_{inc}$$

The coherent and incoherent cross sections for neutron scattering allow recognizing various properties of condensed matter. Coherent scattering gives the information about the equilibrium structure, crystal structure excitation or magnetic subnet excitation. Incoherent scattering describes single atoms or molecules, for example its diffusion in the crystal.

3. Methods

3.1 X-ray diffraction

X-ray scattering techniques are a family of non-destructive analytical techniques which reveal information about the crystal structure, chemical composition, and physical properties of materials and thin films. These techniques are based on observing the scattered intensity of an X-ray beam hitting a sample as a function of incident and scattered angle, polarization, and wavelength or energy. Note that X-ray diffraction is now often considered a sub-set of X-ray scattering, where the scattering is elastic and the scattering object is crystalline, so that the resulting pattern contains sharp spots analyzed by X-ray crystallography (as in the Figure 5). However, both scattering and diffraction are related general phenomena and the distinction has not

always existed. Thus Guinier's classic text from 1963 is titled "X-ray diffraction in Crystals, Imperfect Crystals and Amorphous Bodies" so 'diffraction' was clearly not restricted to crystals at that time.

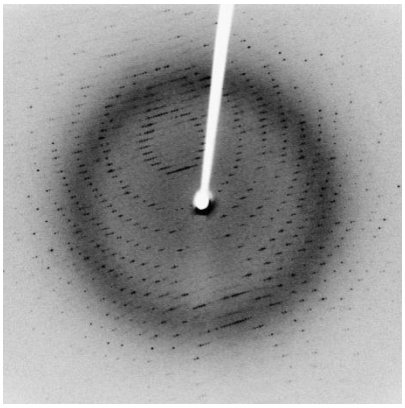

Fig.5. This is an X-ray diffraction pattern formed when X-rays are focused on a crystalline material, in this case a protein. Each dot, called a reflection, forms from the coherent interference of scattered X-rays passing through the crystal [9].

A key element in the formation of many physical, including magnetic, powder properties is their structural state. It it is characterized by the presence of a certain order (or disorder) in the arrangement of atoms at distances comparable to interatomic distances (atomic structure), as well as the size, shape and location of larger-scale formations (microstructure). The most common technique used to study the structural elements of the powder is x-ray diffractometry. X-ray diffraction analysis is based on obtaining and analyzing the diffraction pattern resulting from the interference of x-rays scattered by electrons of the atoms of the irradiated object. If x-rays fall on an ordered system of atoms, the waves scattered by different atoms of such a system and propagating in one particular direction, interfere with each other. Each crystal is an ordered system of atoms or a set of atomic planes. Thus, from the crystal of any substance can be obtained characteristic of his x-ray diffraction pattern. At angles of incidence satisfying the Woolf-Bragg condition:

$$2d \sin \theta_{\text{Б}} = n\lambda$$

the formation of a diffraction wave of high intensity. Here λ is the wavelength of radiation and d is the interplanar distance. According to the Woolf - Bragg condition, diffraction maxima are obtained only at certain directions and interplanar distances.

The method of x-ray reflectometry is based on the registration and analysis of the diffraction pattern from x-rays reflected by the sample at small ($\theta = 0.1 - 5^{o}$) angles of incidence. At angles of incidence less than the critical $\theta < \theta_{K}$, the incident beam is completely reflected by the sample surface. The critical angle for most materials is $\theta K < 0.3^{o}$. The value of the critical angle it is possible to estimate the average density $\boldsymbol{\rho}$ of a substance sample $\theta_{к} \sim \rho^{1/2}$. At angles of incidence greater than the critical value $\theta > \theta_{к}$ x-ray radiation penetrates into the sample. Rays reflected from different interfaces interfere with each other, and as a result, the diffraction pattern is registered oscillations of the intensity (cassig oscillations). The oscillation period $\Delta\theta$ is determined by the film thickness: $\Delta\theta \approx \lambda/(2d)$, where d is the film thickness, λ is the x-ray wavelength. The

decrease in the intensity of oscillations is associated with the roughness of the layers. The higher the perfection of the surface and interfaces, the greater the range of angles observed cassig oscillations.

The method of x-ray reflectometry is to measure the mirror reflection coefficient of x-ray radiation as a function of the transmitted photon pulse $\boldsymbol{q}$. The structure of the sample is determined, as a rule, by fitting (modeling) the experimental curve of the model, which includes parameters describing the structure of the sample. Thus, the fitting of the experimental curves allows to restore the structural profile of the sample. Processing of the traces is carried out using the program PANalytical X'pert Reflectivity. An algorithm for the numerical solution of the mirror reflection problem from an arbitrary potential was proposed by Parrot. An arbitrary potential hetero structure is considered as a sequence of rectangular potentials, i.e. the structure is considered as a N homogeneous throughout the depth of the films with a thickness of $\boldsymbol{z_j}$ with the reflection coefficient $\boldsymbol{r_j}$ and $\boldsymbol{z}$-component of the transferred momentum $\boldsymbol{q_{zj}}$, roughness and imperfection of the boundaries is described by the introduction of additional sublayers. Based on the condition of preservation of the tangential component of the wave vector at the interface of the Parrot, a recurrent ratio for the reflection coefficient was obtained:

$$R_j = \frac{r_j + R_{j+1} e^{2i\varphi}}{1 + r_j R_{j+1} e^{2i\varphi}}$$

where $\boldsymbol{r_j}$ is the Frenel reflection coefficient at the boundary between j_1 and j layer, and $\boldsymbol{R_{j+1}}$ is the reflection coefficient from the boundary between $\boldsymbol{j}$ and $\boldsymbol{j+1}$ layers. Iterations start from the substrate, downwards j, to j=0, the substrate is considered semi-infinite, which means $\boldsymbol{R_{j+1}} = 0$.

3.2 Inelastic neutron scattering

The investigation method being used in the scientific team in which I worked is inelastic *incoherent neutron scattering*. To study this method it is indispensable to know about different kinds of neutron scattering. The first one is *elastic neutron scattering*. It is when a neutron beam incident on a fixed, point scattered like nucleus and there is no change in the energy of the incident neutron. Although the direction of the wave vector of the neutron changes, its magnitude does not. The example of this kind of scattering is *diffraction*. When neutrons are scattered by matter, the scattering from each of the individual nuclei are added. Nuclei are not fixed because atoms in matter undergo atomic vibrations. Nuclei can also recoil during a collision with a neutron. As nuclei are moving they can impart or absorb energy of neutrons. This kind of neutron scattering is named *inelastic neutron scattering* and in this process the direction and the magnitude of the neutron wave vector change (Fig.6).

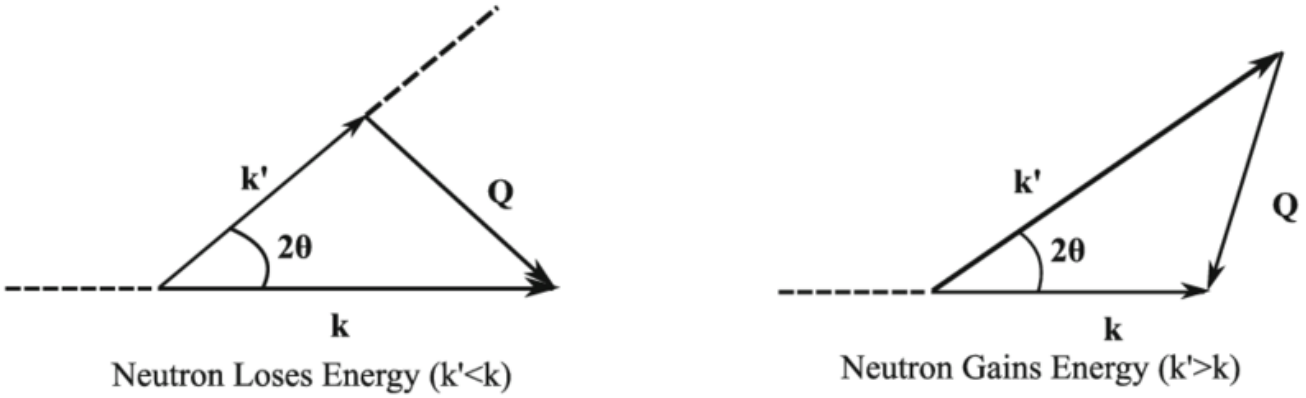

Fig.6. Inelastic Scattering [10].

These two types of neutron scattering provide different scattering effects. So we are talking about *coherent neutron scattering* when the neutron wave interacts with the whole sample as a unit and then the scattered waves from different nuclei interfere with each other. As this type of neutron scattering depends on the relative distances between the constituent atoms, it gives the information about the structure of materials.

In incoherent neutron scattering an incident neutron wave interacts independly with each nucleus so that the scattered waves have indeterminate relative phases and they do not interfere with each other. However, the intensities from each nucleus add up.

To investigate the neutron scattering it is indispensable to get to know about the *phonons* and *magnons*. As we know, in reality atoms are not frozen in fixed positions in a crystal. As they have thermal energy, they oscillate about their lattice site and move around inside a small volume with the lattice site at its centre. We can name this position in the centre the official position. As atoms are connected with each other by the binding forces, when one atom oscillate, neighboring atoms also start to oscillate with different frequencies and wavelength travelling in different directions. In effect they form the wave, which starts passing up and down. There are many waves like that which are formed by these thermal motions of atoms. We can describe the superposition of this waves mowing through the lattice. These fundamental vibrational waves in a crystal in which nuclei oscillate in a coordinated manner are named *phonons.* The energy of phonons is quantized and has a υ that is the frequency of atomic motion associated with the phonon.

Besides the neutron interaction with atomic nuclei, there is also an interaction between a neutron and the magnetic field from the fact that a neutron has a magnetic moment. The neutron experiences this magnetic force, when it passes near the electron. As most electrons in atoms are paired, they do not have the magnetic moment, but in some other atoms there are no paired electrons from valence shell. So neutrons could be also scattered by the resulting magnetic moments. It happens for example in ferromagnetic and antiferromagnetic materials, which have aligned magnetic moments of their electrons (in ferromagnetic they are pointed in the same direction and in antiferromagnetic in opposite directions). In the neutron scattering only the component of the sample's magnetization that is perpendicular to the scattering vector, is effective. As in magnetized

materials the directions of the atomic moments can oscillate, they form a wave of magnetic oscillation that passes through the sample. These magnetic excitations are called *magnons.* Thus, they are magnetic analogues of the phonons and can be measured by the inelastic neutron scattering.

Returning to the inelastic incoherent neutron scattering the double differential cross section for incoherent neutron scattering will be [11]:

$$\frac{d^2\sigma}{d\Omega d\omega} = \frac{k_1}{k_0}\sum_i (b_i^{inc})^2 S^{inc}(\vec{Q}, \omega)$$

where the k_0 and k_1 are the wave vector of incident and scattered (relatively) neutron wave and $S^{inc}(\vec{Q}, \omega)$ is the incoherent scattering law. Mathematically it is a spatial and time Fourier transformation of autocorrelation function, which describes the probability that the atom being at one point in time *t=0* will be found at a second definite point in time *t.* Thus, this method allows investigating nanoparticlesdynamics effects like:

- local and quasilocal vibrations of admixtures,
- crystal field splitting,
- intramolecular vibrations,
- phonons and magnons density of states.

In spectroscopic studies of intramolecular vibrations of molecules containing hydrogen atoms we can say that in the scattering law there are only the vibrations of hydrogen. It is because for hydrogen there is a big value of a scattering length. It gives an equation for the scattering law [11]:

$$S(Q, n\omega) = \frac{1}{n!}(Q^2 < U^2 >)^n \exp(-Q^2 < U^2 >)$$

where $<U^2>$ is an average value of a square vibration amplitude and *n* is the principal quantum number. For *n=0* this equation describes the dependence of the intensity of neutron scattering from *Q.* For *n=1* it describes the first excited state of oscillator. The neutron scattering is analogic to the optical spectroscopy. But there are differences, which make this method an important complement for optical spectroscopy. Firstly there are no selection rules. Secondly, the signal intensity is proportional to *U* meanwhile for optic spectroscopy it is not. Furthermore, the large amplitude of hydrogen vibrations and the anomaly large cross section for neutron scattering makes the neutron spectroscopy an unusually sensitive method for investigating the samples containing hydrogen atoms. As we know, deuter does not have that large cross-section, so by changing the hydrogen atom for deuter, we can define the type of vibrations that corresponds to the signals in neutron spectrum. Finally, these materials, which are not transparent for visible and infrared spectrum, are transparent for neutrons (e.g. metals).

The inelastic incoherent neutron scattering is also used in the studies of phonons density of states - *g(ω)*. This function characterizes the probability that the vibrational waves with the frequency *ω* will exist in a

crystal. For compounds containing hydrogen atoms the cross section for incoherent scattering will be described by [11]:

$$(\frac{d^2\sigma}{d\Omega d\omega})_{inc} = \frac{k_1}{k_0} N \frac{|Q^2|}{4\omega M} (b_H^{inc})^2 e^{-2W} G_H(\omega) (cth \frac{\hbar\omega}{2kT} \pm 1)$$

where *M* is the mass of crystal unit cell and $G_H(\omega)$ is the phonons density of states for hydrogen.

3.3 Neutron diffraction

Neutron diffraction or elastic neutron scattering (Fig.7) is the application of neutron scattering to the determination of the atomic and/or magnetic structure of a material.

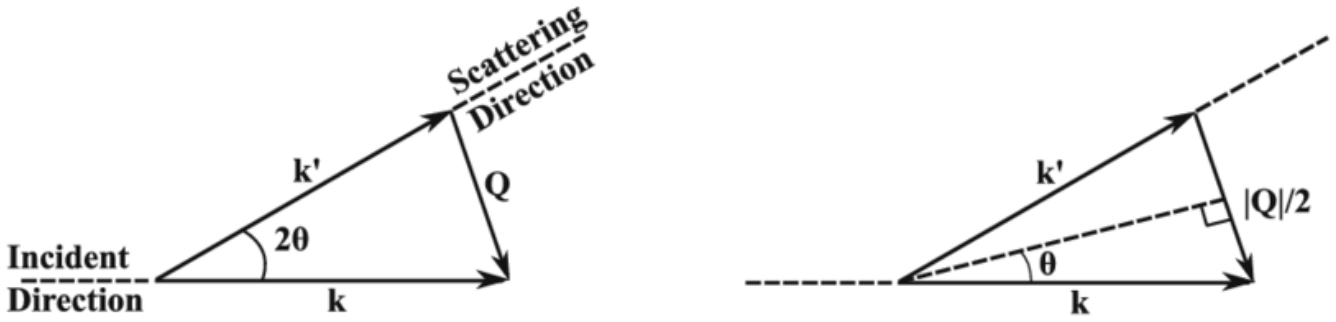

Fig.7. Elastic Scattering [10].

A sample to be examined is placed in a beam of thermal or cold neutrons to obtain a diffraction pattern that provides information of the structure of the material. The technique is similar to X-ray diffraction but due to their different scattering properties, neutrons and X-rays provide complementary information: X-Rays are suited for superficial analysis, strong x-rays from synchrotron radiation are suited for shallow depths or thin specimens, while neutrons having high penetration depth are suited for bulk samples.

Like all quantum particles, neutrons can exhibit wave phenomena typically associated with light or sound. Diffraction is one of these phenomena; it occurs when waves encounter obstacles whose size is comparable with the wavelength. If the wavelength of a quantum particle is short enough, atoms or their nuclei can serve as diffraction obstacles. When a beam of neutrons emanating from a reactor is slowed down and selected properly by their speed, their wavelength lies near one angstrom (0.1 nanometer), the typical separation between atoms in a solid material. Such a beam can then be used to perform a diffraction experiment. Impinging on a crystalline sample, it will scatter under a limited number of well-defined angles, according to the same Bragg's law (Fig.8) that describes X-ray diffraction.

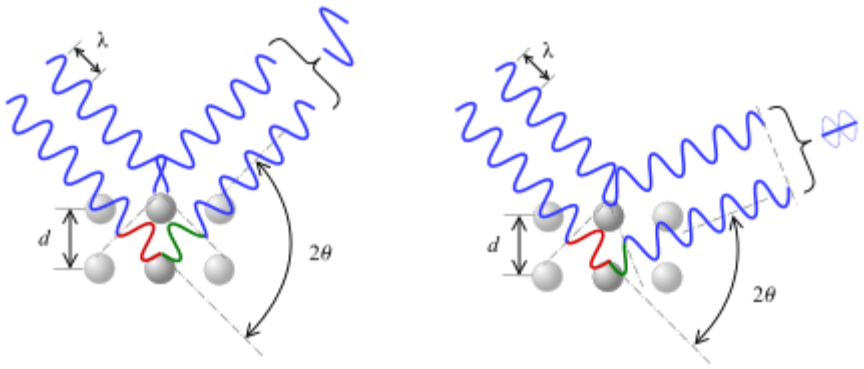

Fig.8. According to the 2θ deviation, the phase shift causes constructive (left figure) or destructive (right figure) interferences [12].

Neutrons and X-rays interact with matter differently. X-rays interact primarily with the electron cloud surrounding each atom. The contribution to the diffracted x-ray intensity is therefore larger for atoms with larger atomic number (Z). On the other hand, neutrons interact directly with the nucleus of the atom, and the contribution to the diffracted intensity depends on each isotope; for example, regular hydrogen and deuterium contribute differently. It is also often the case that light (low Z) atoms contribute strongly to the diffracted intensity, even in the presence of large Z atoms. The scattering length varies from isotope to isotope rather than linearly with the atomic number. An element like vanadium strongly scatters X-rays, but its nuclei hardly scatters neutrons, which is why it is often used as a container material. Non-magnetic neutron diffraction is directly sensitive to the positions of the nuclei of the atoms.

The nuclei of atoms, from which neutrons scatter, are tiny. Furthermore, there is no need for an atomic form factor to describe the shape of the electron cloud of the atom and the scattering power of an atom does not fall off with the scattering angle as it does for X-rays. Diffract grams therefore can show strong, well-defined diffraction peaks even at high angles, particularly if the experiment is done at low temperatures. Many neutron sources are equipped with liquid helium cooling systems that allow data collection at temperatures down to 4.2 K. The superb high angle (i.e. high resolution) information means that the atomic positions in the structure can be determined with high precision. On the other hand, Fourier maps (and to a lesser extent difference Fourier maps) derived from neutron data suffer from series termination errors, sometimes so much that the results are meaningless.

Although neutrons are uncharged, they carry a magnetic moment, and therefore interact with magnetic moments, including those arising from the electron cloud around an atom. Neutron diffraction can therefore reveal the microscopic magnetic structure of a material.

Magnetic scattering does require an atomic form factor as it is caused by the much larger electron cloud around the tiny nucleus. The intensity of the magnetic contribution to the diffraction peaks will therefore decrease towards higher angles. Neutron diffraction can be used to determine the static structure factor of

gases, liquids or amorphous solids. Most experiments, however, aim at the structure of crystalline solids, making neutron diffraction an important tool of crystallography.

Neutron diffraction is closely related to X-ray powder diffraction. In fact, the single crystal version of the technique is less commonly used because currently available neutron sources require relatively large samples and large single crystals are hard or impossible to come by for most materials. Future developments, however, may well change this picture. Because the data is typically a 1D powder diffractogram they are usually processed using Rietveld refinement. In fact the latter found its origin in neutron diffraction (at Petten in the Netherlands) and was later extended for use in X-ray diffraction.

One practical application of elastic neutron scattering/diffraction is that the lattice constant of metals and other crystalline materials can be very accurately measured. Together with an accurately aligned micropositioner a map of the lattice constant through the metal can be derived. This can easily be converted to the stress field experienced by the material. This has been used to analyze stresses in aerospace and automotive components to give just two examples. The high penetration depth permits measuring residual stresses in bulk components as crankshafts, pistons, rails, gears. This technique has led to the development of dedicated stress diffractometers, such as the ENGIN-X instrument at the ISIS neutron source.

Neutron diffraction can also be employed to give insight into the 3D structure any material that diffracts.

4. Experiment

4.1 X-ray diffractometer

All x-ray measurements were performed on a laboratory x-ray diffractometer PANalytical Empyrean Series 2 (Figure 9). The basis of the Empyrean system consists of the following elements:

- the case of the diffractometer and the electronics unit;
- goniometer, Central part of the diffractometer (2);
- x-ray tube in the tube body mounted on the goniometer (6);
- optical modules for incident and diffracted x-ray beam (1 and 3);
- platform for the sample on which the sample is installed to measure its characteristics (5);
- detector for measuring the intensity of the diffracted x-ray beam (4).

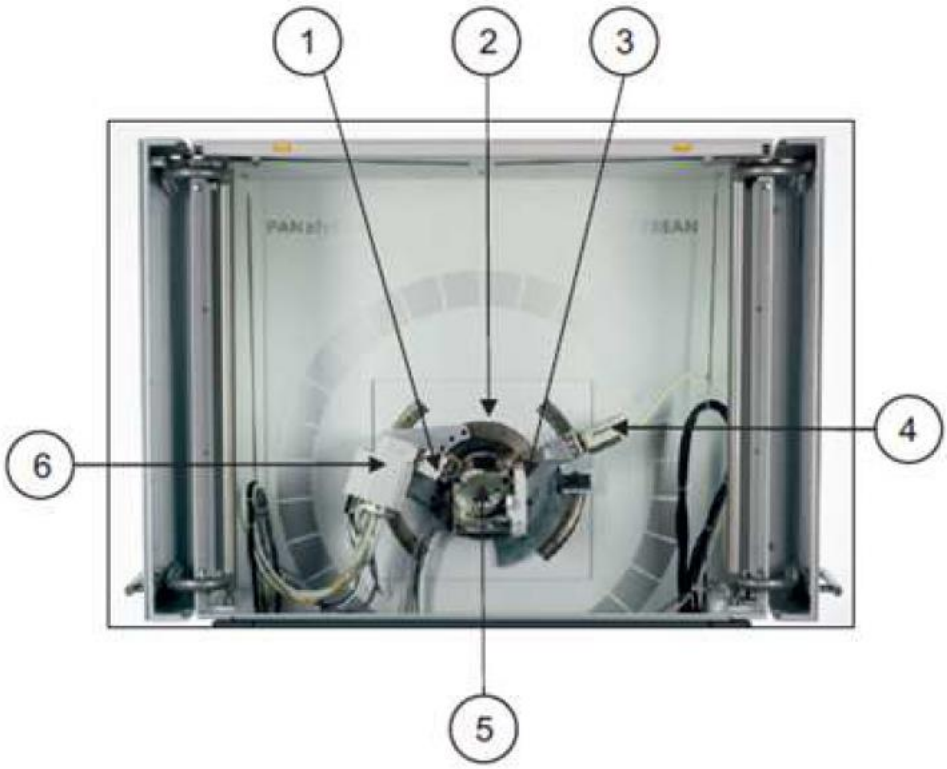

Fig.9. Photo and diagram of PANalytical Empyrean diffractometer [13].

This diffractometer equipped with an x-ray tube with a water-cooled anticathode made of copper (chromium, molybdenum, cobalt, etc.). In the bombardment of the accelerated electrons-cathode copper $K_{\alpha 1}$ emits a spectral line with a wavelength of 1.54 Å. A proportional (scintillation) counter is used as an x-ray detector. The operation of the proportional counter is based on the phenomenon of gas amplification. Gas amplification is an increase in the number of free charges in the volume of the detector due to the fact that the primary electrons on their way to the anode in large electric fields acquire energy sufficient for the shock ionization of neutral atoms of the working medium of the detector. The resulting new electrons, in turn, have time to acquire energy sufficient for ionization by impact. Thus, an increasing electronic avalanche will move to the anode. This "self-amplification" of the electronic current (gas gain) can reach 103 -104 . This mode of operation corresponds to the proportional counter (camera). The name reflects the fact that in this device the amplitude of the current pulse (or the total charge collected) remains proportional to the energy expended by the charged particle on the primary ionization of the detector medium. Thus, the proportional counter is able to perform the functions of a spectrometer, as well as an ionization chamber. The energy resolution of proportional meters is better than that of scintillation meters, but worse than that of semiconductors. To measure the sample is mounted on a horizontal platform, which is mounted on the turntable goniometer. The mechanical system of the goniometer is driven by stepper motors, which are controlled by a microcontroller.

The diffractometer is connected to a computer where a special data Collector program is installed. Control software allows in automatic mode to remove the trace.

4.2 NERA spectrometer

The NERA Group is a part of Frank Laboratory of Neutron Physics of the Joint Institute for Nuclear Research in Dubna. The NERA spectrometer is aimed to study inelastic and quasielastic neutron scattering with simultaneous control of the phase of the sample by neutron diffraction. This spectrometer is used to investigate the dynamics and structure of condensed matter.

The NERA spectrometer is an inverse geometry time-of-flight spectrometer. In this type of spectrometer a pulsed neutron source produces the polychromatic neutron beams with the period *T*. They have continuous energy spectrum and their energy $E_i$is appointed from the time of flight measured between a source and a sample. The energy of scattered neutrons is monochromated by a monochromator placed after the sample. The detectors are placed at different angles that provides recording of spectra for different values of scattering vector $\vec{Q}$and for the same value of ω. The time-of-flight will be given by the equation below:

$$t_i = t - \frac{(L_{f1} + L_{f2})}{v_f}$$

where *t* is unrestricted time from the neutron beam generation, L_{f1} and L_{f2} are the distances between a sample and a monochromator and a detector relatively,$v_f = \sqrt{\frac{2E_f}{m}}$ is the velocity of scattered nautrons determined by crystal. Thus, the neutron energy will be [11]:

$$E_i = \frac{m}{2}\left(\frac{L_i}{t - \frac{L_{f1}+L_{f2}}{v_f}}\right)^2$$

Where L_i is the neutron time-of-flight from the source to the sample.

The spectrometer and its description is presented in Figure 10.

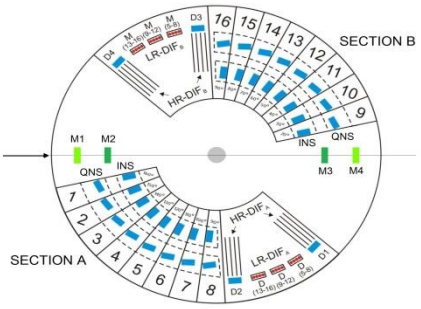

A

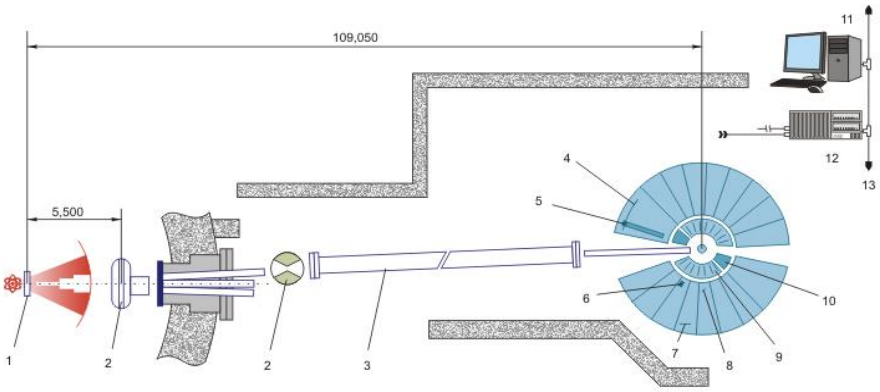

B

Fig.10. NERA spectrometer [14].

The produced neutron beam is slowed in the moderator (1) and background choppers (2) remove the background. After that, the neutron beam goes throw the neutron guide (3). The neutron beam incident on the sample (11). A spectrometer has 2 parts, each with 8 sections for measuring the inelastic scattering and one for the elastic scattering. The 4 and 5 are the diffraction detectors and (7) is a single crystal quasielastic neutron scattering analyzer. For the inelastic incoherent neutron scattering the devices are used: ^{3}He Detectors (6) Pyrolytic Graphite INS Analyzer (8), Be-filters (9) and collimators (10). At the same time 16 INS spectra are registered at angles from 20^{o} to 160^{o}. Be-filters are cooled in liquid nitrogen.

5. Results and discussion

X-ray diffractometer

We carried out experiments on PANalytical Empyrean X-ray diffractometer as follows:

- Initially, the samples were prepared for the experiment
- placed on a diffractometer
- DATA COLLECTOR program launches a diffractometer
- The results obtained are processed in FullProf or HighScore program

We performed the measurements for a few samples: pristine multiwall carbon nanotubes (MWNT) from Nanocyl S.A., modified multiwall carbon nanotubes, pure doxorubicin and doxorubicin onto modified MWNT. Multi-wall carbon nanotubes were modified via treatment in boiling nitric acid. The acid treatment leached the residual catalyst particles and introduced surface functional groups which have acidic properties. The presence of functional groups on the CNT surface allows to adsorb more doxorubicin compared to unmodified carbon nanotubes.

The X-ray result for pristine MWNT is presented in Figure 11.

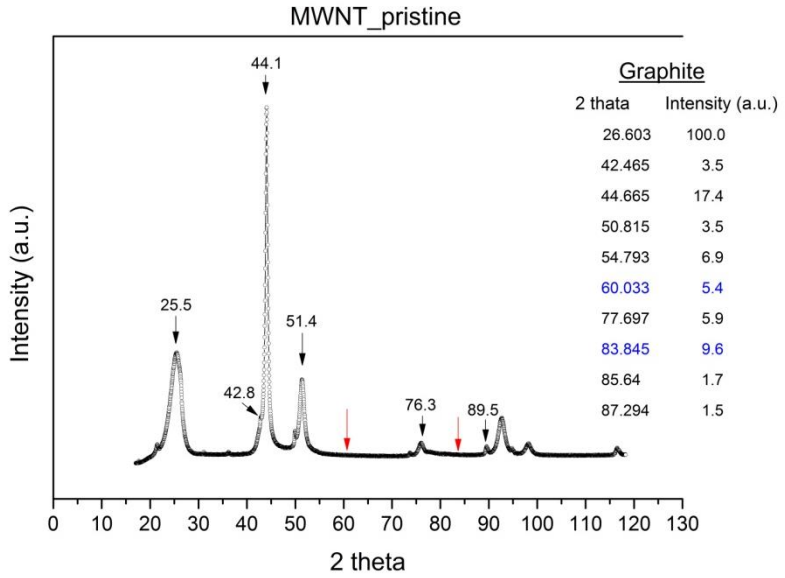

Fig.11. X-ray result for pristine MWNT at 295K.

Carbon nanotubes (CNTs) are tubes made of carbon which formed by rolling up a sheet of graphene. If there are multiple sheets of graphene which are rolling up the multiwalled carbon nanotubes are obtained, see Figure 12.

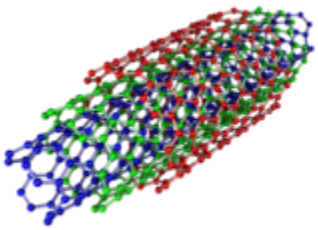

Fig.12. Illustration of MWNT [15].

Due to the fact that MWNT are formed by rolling up the graphene sheets the structure of our MWNT have been compared with the graphite structure [Mincryst database] which is presented in Fig.11. As we can see in Fig.11 some of graphite diffraction peaks are the same position as MWNT but there are also some

differences as well as positions of the peaks and their intensities. This result we can conclude that measured MWNT are not the same structure as graphite. It may be due to some defects of carbon walls as the vacancies and dislocations or different structure at the ends of tubes (the ends of the tubes are probably closed).

X-ray measurements show also that the structure of MWNT pristine and modified MWNT is almost the same which is presented in Fig.13.

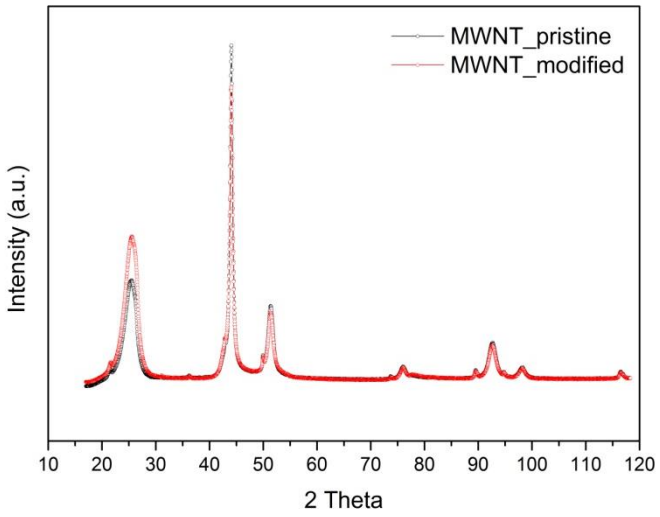

Fig.13. X-ray results for pristine and modified MWNT at 295K.

The results presented in Fig.13 show the small differences in the peaks intensities. These results means that wall modification by acid treatment of MWNT do not change the structure of carbon nanotubes.

The X-ray studies was also carried out for pure doxorubicin (DOX) and obtained result is presented in Figure 14.

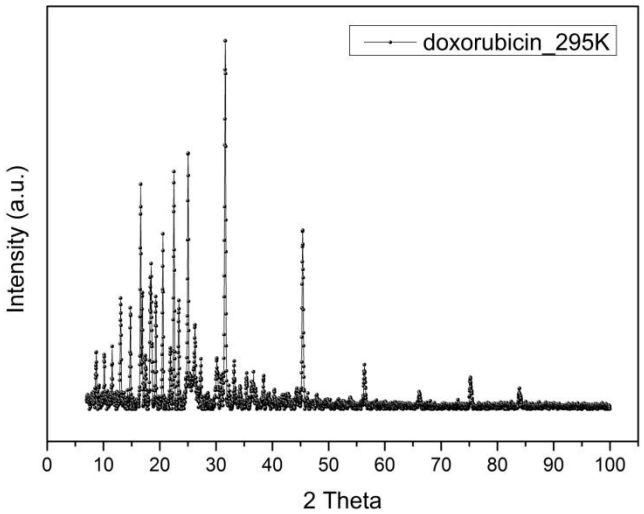

Fig.14. X-ray result for doxorubicin at 295K.

As it was shown in Fig. 14 the structure of doxorubicin consist of many diffractional peaks. It can be interpreted that doxorubicin crystallizes into a structure with low symmetry. Unfortunately due to the lack of the structural details of doxorubicin in available database we could not analyze the experimental result for this sample by use the program like for example FullProf.

The most interesting was to measure the structure of doxorubicin onto modified MWNT. The X-ray results for doxorubicin onto MWNT at two different temperatures are presented in Figure 15.

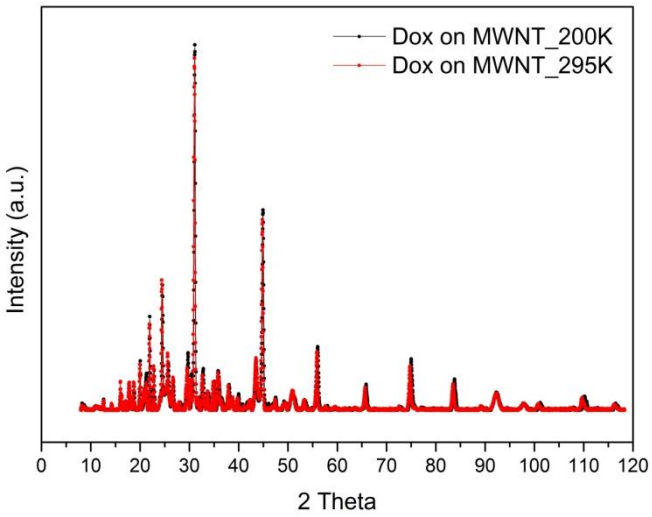

Fig.15. X-ray results for doxorubicin onto modified MWNT at 200K and 295K.

The results obtained for doxorubicin onto modified MWNT at different temperature suggest that the structure of this sample is almost the same in wide range of temperatures.

The comparison of the structure of pure doxorubicin and doxorubicin onto modified MWNT (Figures 16) indicates that for small values of angles, the intensity and positions of the peaks were changed significantly. This result is not clear and requires further research and analysis.

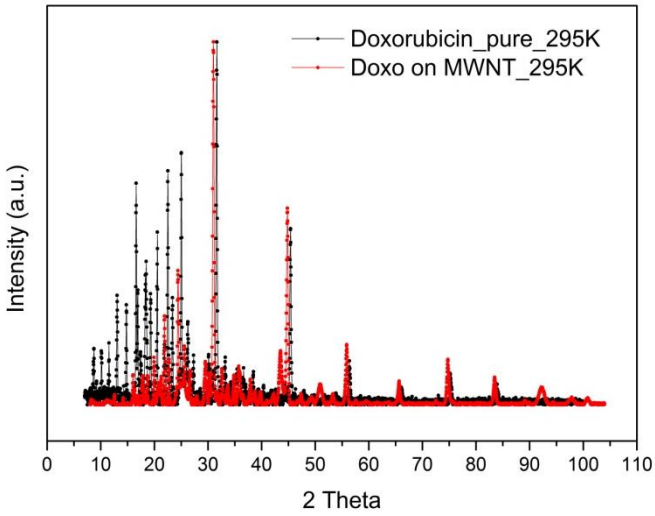

Fig.16. X-ray results for pure doxorubicin and doxorubicin onto modified MWNT at 295K.

Neutron scattering results

The neutron diffraction experiments were carried out on the NERA spectrometer:

- before the measurements the samples were prepare to the ND experiments
- collected data were analyzed in Nuvis program

As the part of the presented work the neutron measurements were also analyzed. In Figure 17 the neutron diffraction results for doxorubicin at 10K are presented.

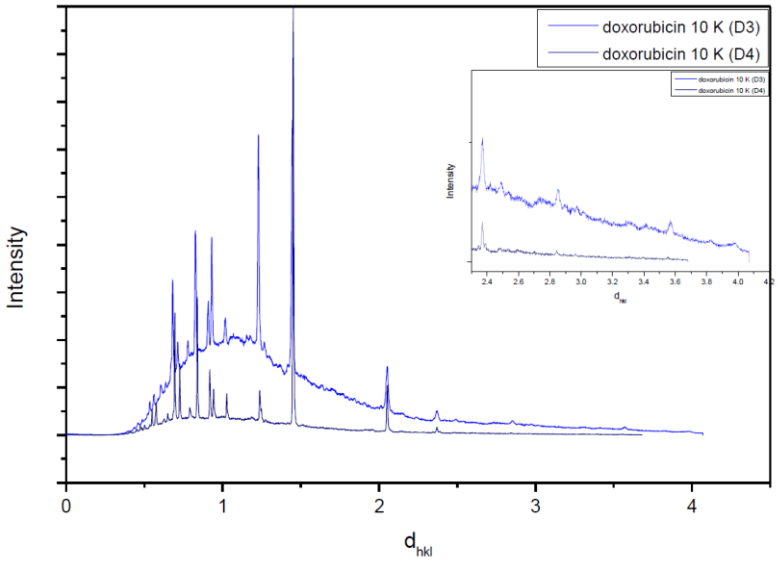

Fig.17. Neutron diffraction result for pure doxorubicin at 10K for two different measuring channels.

The sharp peaks visible in Fig.17 are related with the container which was using in experiment and are typical for aluminum structure. Diffraction peaks connected with the sample are much smaller than the peaks come from aluminum and are primarily visible in the range of interplanar spacing, d_{hkl}, from 2 to 4 Å. As expected, the diffraction spectra are the same for different channels.

The ND results for doxorubicin at 295K are presented in Figure 18. As in the case of spectra obtained at 10K the diffraction peaks come from measuring container are visible. There are also some peaks connected with the structure of doxorubicin.

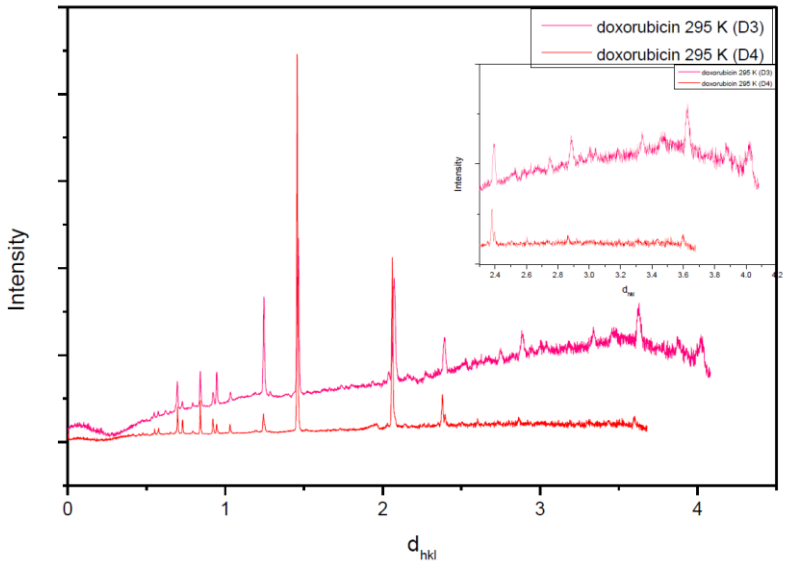

Fig.18. Neutron diffraction result for pure doxorubicin at 295K for two different measuring channels.

In Figures 19 and 20 we presented the comparison of ND measurements for doxorubicin at two different temperatures, 10K and 295K, respectively.

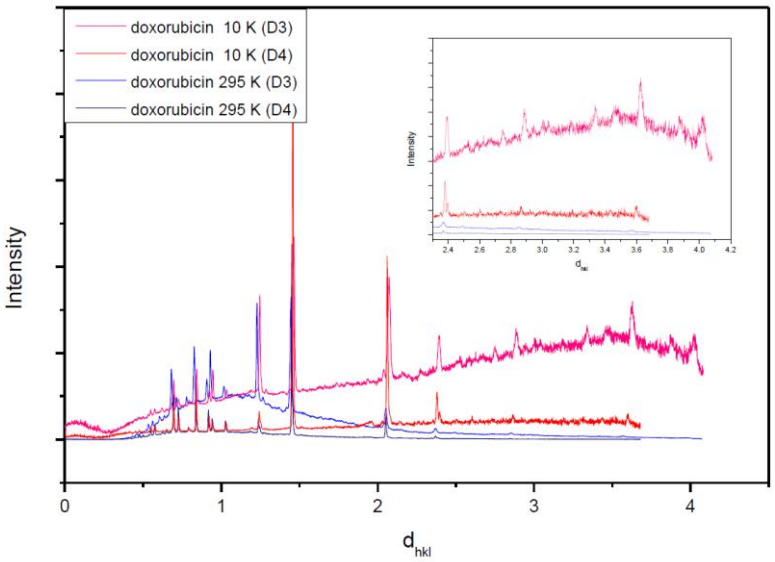

Fig.19. Neutron diffraction results for pure doxorubicin at two different temperatures 10K and 295K.

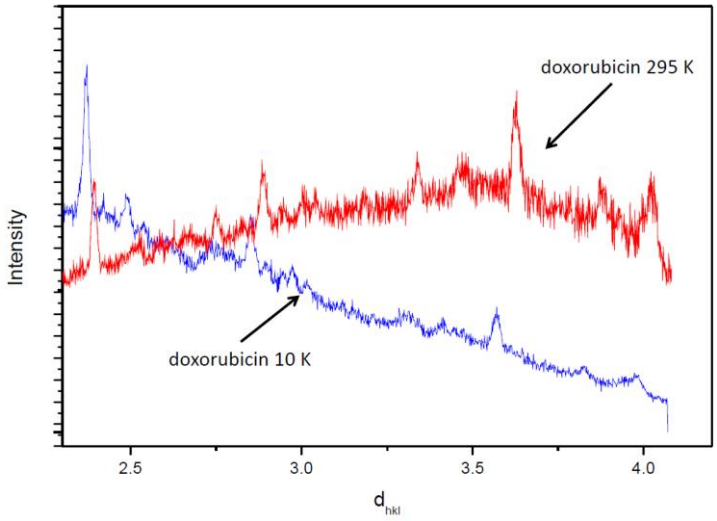

Fig.20. Neutron diffraction results for pure doxorubicin at two different temperatures 10K and 295K at the range of d_{hkl} from 2Å to 4Å.

The obtained results suggest that there are not significant changes in structure of doxorubicin at wide range of temperatures. It is difficult to describe the structure of the sample based on results which were obtained.

6. Conclusion

The structure of doxorubicin was analyzed based on ND and X-ray measurements. X-ray studies were carried out for both pristine and modified multiwalled carbon nanotubes. The obtained results suggest that the structure of MWNT is not typical graphite structure but has a structure similar to graphite. What's more, based on the performed studies, it can be said that the structure of modified and non modified MWNT is the same. X-ray technique was also use to describe the structure of pure doxorubicin and doxorubicin onto MWNT. The structure of analyzed samples is the same at 200K and 295K. Based on obtained results can also be seen that the structure of pure doxorubicin and doxorubicin onto modified MWNT is a little different which seems to be logical. ND results were shown that the structure of doxorubicin at 10K and 295K is similar. There are difficulties to describe the experimental structure of doxorubicin due to the lack of theoretical parameters for this substance.

7. Acknowledgement

We would like to convey our gratefulness to our supervisor in this Summer Student Program, dr. Dorota Chudoba. First of all for accepting us as a student, and also, for her patience, her support and the excellent guidance. The knowledge that we have gained throughout this eight week we perceive as highly valuable component in our future career development.

Especially, we would like to thank our supervisor in Uzbekistan, Ibragimova Elvira Memetovna and Bekmirzayev Rakhmatilla, for encouraging us and supporting us to take part in the Program. Also, We would like to thank the Joint Institute for Nuclear Research for giving us the opportunity to participate in the Summer Student Program and for financial support. Stay in Dubna was one of the best adventures in our life.

We are also grateful to INP AS RUz staff Yakhub Akhmedov, Ulughbek Kurbanov and the staff of the JINR FLNP Bekhzodjon Abdurakhimov, Kahramon Mamatqulov and members of group of NERA for useful discussions.

Lastly, we also thank our family for always supporting us in all possible ways.

8. References

[1]. http://flnph.jinr.ru/en/education/properties-of-neutrons

[2]. https://upload.wikimedia.org/wikipedia/commons/thumb/8/81/Quark_structure_neutron.svg/ 2000px-Quark_structure_neutron.svg.png

[3]. https://en.wikipedia.org/wiki/Free_neutron_decay

[4]. Carlile C.J., Lectures on Neutron Scattering Techniques.1. The production of neutrons, Rutherford Appleton Laboratory Report RAL-88-070.UK.1988

[5]. R. Celotta, J. Levine, Methods of Experimental Physics. Neutron Scattering, Academic Press, INC, London 1986

[6]. http://www.nucler-power.net/wp-content/uploads/2014/10/nucler_fission.jpg?32b4fc

[7]. http://flnp.jinr.ru/251/

[8]. Bee M., Quasielastic Neutron Scattering. Bristol and Philadelphia: Adam Hilger, 1988; А.В. Белушкин, Основы исследований свойств конденсированных сред с помощью рассеяния нейтронов Дубна 2010

[9]. https://en.wikipedia.org/wiki/Xray_scattering_techniques

[10]. https://yandex.ru/images/search?from=tabbar&text=Inelastic%20Scattering

[11]. Shirane G, Shapiro S.M, Tranquada J.M, Neutron Scattering with a Triple-Axis Spectrometer: Basic Techniques. Cambridge, 2002

[12]. https://en.wikipedia.org/wiki/Bragg%27s_law

[13]. http://www.imp.uran.ru/sites/default/files/upload/otchet-2016.pdf

[14]. http://nuvis.jankrawczyk.pl, http://flnph.jinr.ru/en/facilities/ibr-2/instruments/nera

[15]. https://en.wikipedia.org/wiki/Carbon_nanotube